

## Plastic flow localization in bulk tungsten with ultrafine microstructure

Q. Wei, K. T. Ramesh, and E. Ma<sup>a)</sup>

Center for Advanced Metallic and Ceramic Systems (CAMCS), The Johns Hopkins University, Baltimore, Maryland 21218

L. J. Kesckes and R. J. Dowding

Army Research Laboratory, Aberdeen Proving Ground, Maryland 21005

V. U. Kazykhanov and R. Z. Valiev

Ufa State Aviation Technical University, Ufa 450000, Russia

(Received 3 December 2004; accepted 14 January 2005; published online 3 March 2005)

Shear localization is demonstrated in bulk tungsten (W) of commercial purity under dynamic uniaxial compression. Microstructure refinement via severe plastic deformation was the strategy used to induce this unusual deformation mode for W. The ultrafine microstructure achieved in bcc materials leads to elevated strength and ductility, as well as reduced strain hardening and strain rate hardening, thus enhancing the propensity for adiabatic plastic flow localization. © 2005 American Institute of Physics. [DOI: 10.1063/1.1875754]

Plastic flow localization in the form of shear banding is an important deformation mode in a wide range of deformation operations, especially at high loading (strain) rates.<sup>1</sup> Applications within which shear localization is of critical importance include explosive fragmentation, high-speed machining, and kinetic energy penetrators.<sup>2–4</sup> However, pure body-centered cubic metals and especially tungsten (W) are notoriously resistant to shear localization because of their strong rate sensitivity. Shear localization in high-density W and W-based alloys has been sought for many years, but such efforts have met with little success, despite the wide range of alloying elements that have been introduced to tailor the phase composition and microstructure.<sup>2,4</sup>

In this letter, we demonstrate a strategy to induce highly localized shear flow in tungsten, based on refining the microstructure of W down to ultrafine scales. Our approach is built upon the following considerations. Under compression, a flow localization parameter,  $\alpha$ , can be used to qualitatively describe the propensity of a metal for flow localization<sup>5,6</sup> (there are other more sophisticated criteria for shear susceptibility under adiabatic or isothermal conditions, but the general principle remains the same<sup>1</sup>). This parameter is a function of two material properties

$$\alpha = (\gamma - 1)/m. \quad (1)$$

The first is the normalized strain-hardening rate,  $\gamma$ , given by  $1/\sigma(\partial\sigma/\partial\epsilon)|_{\dot{\epsilon}}$ , in which the thermal softening effect can be included. Here  $\sigma$  is the flow stress,  $\epsilon$  the strain, and  $\dot{\epsilon}$  the strain rate. In compressive loading, a positive  $\gamma$  corresponds to flow softening in the true stress versus true strain curve. The other parameter is the strain rate sensitivity of the flow stress,  $m$ , which is defined as  $m = \partial \ln \sigma / \partial \ln \dot{\epsilon}$ . An increased  $\alpha$  (the result of a more positive  $\gamma$  and/or a smaller  $m$ ) leads to increased tendency for flow localization due to the suppression of the stabilizing mechanisms of strain hardening and strain rate hardening; softening mechanisms (thermal or geometric) can then take over to allow plastic strains to be concentrated in local regions. In the following, we demonstrate

the strong effects of ultrafine W microstructure on  $\gamma$  and  $m$ , as well as the *first* observation of shear localization in bulk W under uniaxial dynamic compressive loading conditions.

Our processing utilized severe plastic deformation (SPD) to decompose the large grains inside the bulk, conventional W (grain diameter  $d$  of several to several tens of micrometers). One procedure started with equal channel angular pressing (ECAP), a technique known to be efficient in refining the grain size of metals and alloys.<sup>7,8</sup> ECAP was conducted at 1100–1000 °C (die angle 120°) for a true strain up to 3, leading to grain refinement ( $d$  to nearly 1  $\mu\text{m}$ ) and improved ductility for further processing. To prevent oxidation and for cooling of the billet during ECAP, a steel covering shell was used.<sup>8</sup> For additional SPD at lower temperatures to store more dislocations and continue the grain refinement, a piece was machined off the ECAP rod and rolled in a confined mode at successively lowered temperatures (with the final rolling at 600 or 700 °C) to an additional true strain of  $\sim 1.8$ . The W is characterized by submicrometer features including grains and subgrains that have sizes of the order of 500 nm, and high densities of dislocations. An example of such ultrafine-grained (UFG) microstructure is shown in the transmission electron micrograph of Fig. 1.

The UFG-W was tested in compression under both quasistatic ( $\dot{\epsilon} \sim 10^{-4} - 10^0 \text{ s}^{-1}$ ) and dynamic ( $\dot{\epsilon} \sim 10^3 \text{ s}^{-1}$ ) loading rates. The dynamic loading was performed using the Kolsky bar or split Hopkinson bar technique as described in Ref. 9. Figure 2 displays the true stress-true strain curves acquired. For these curves, the final load drop is due to unloading at a prescribed strain level. The UFG-W samples have simultaneously high strength and good ductility in both the quasistatic and high-rate tests. The high strength of  $\sim 2.5 \text{ GPa}$  is about 2.5 times that of coarse-grained W at quasistatic rates<sup>10,11</sup> and is desirable for kinetic energy penetration applications. Also, upon dynamic loading of a high strength material, the large plastic work can be converted into heat and thus is favorable for adiabatic shear banding.<sup>1</sup> While commercial polycrystalline W is well known to have limited ductility,<sup>12</sup> the SPD processed UFG-W showed no premature (or preexisting) cracking that would otherwise preempt plastic flow localization.

<sup>a)</sup> Author to whom correspondence should be addressed; electronic mail: ema@jhu.edu



FIG. 1. Transmission electron micrographs of SPD-processed UFG-W, showing grains and dislocation cell structures refined to sizes of the order of 500 nm.

The UFG-W behaves in an elastic-nearly perfect plastic manner under quasistatic loading, as seen from the nearly flat stress-strain curves after yielding. This indicates that the high-density of defects produced during SPD has greatly reduced the strain hardening rate of the commercial polycrystalline W. Under dynamic loading, the UFG-W actually exhibited effective flow softening (Fig. 2), i.e., a positive  $\gamma$  as desired in Eq. (1). This is a result of the temperature rise during the dynamic tests from dissipated plastic work.

The rate sensitivity  $m$  has been evaluated by making double logarithmic plots of the flow stress data recorded at a number of strain rates, at a fixed strain below 0.1.<sup>13</sup> An early work reported  $m=0.042$  for recrystallized W.<sup>14</sup> This  $m$  is approximately cut in half for the UFG-W, Fig. 3. This reduction in  $m$  can be explained by considering the thermally activated deformation mechanism in bcc metals at low homolo-

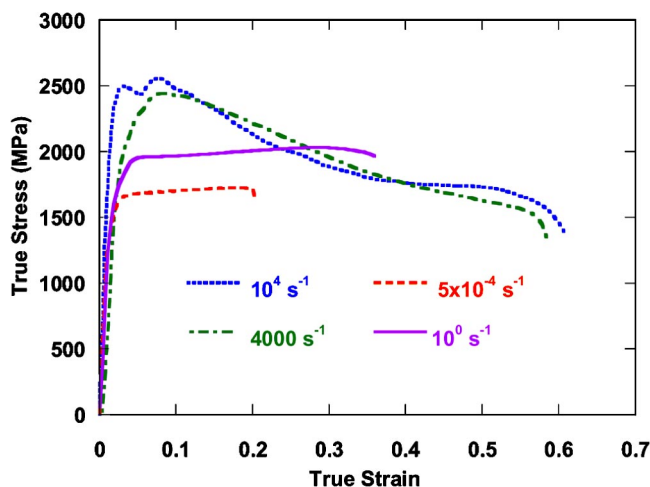


FIG. 2. (Color online). True stress-strain curves of the UFG-W rectangular samples with square loading faces. The quasistatic tests used strain rates  $\sim 10^{-4}$ – $10^0$   $s^{-1}$  (MTS servohydraulic system). The specimens had a height to width ratio close to 2, following American Society for Testing and Materials standards. The dynamic (Kolsky bar) testing at high rates of  $10^3$ – $10^4$   $s^{-1}$  used samples with a height to width ratio  $>0.6$  but  $<1$ , following well-established protocol (see Ref. 9).

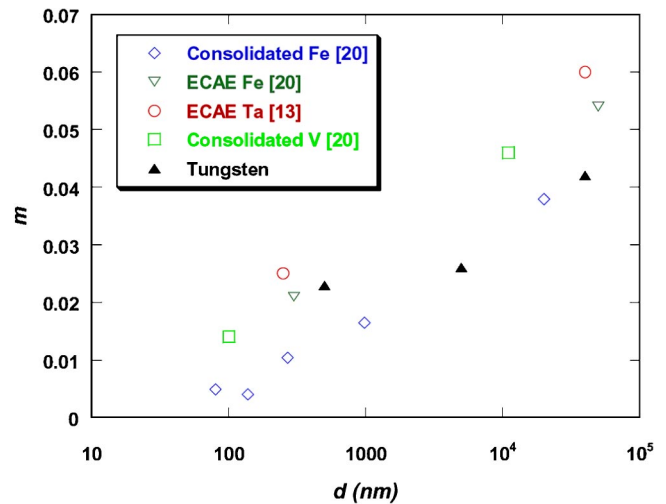


FIG. 3. (Color online). Strain rate sensitivity,  $m$ , is reduced monotonically with microstructure refinement into the UFG regime, in several bcc metals (Fe, Ta, V, open symbols). The values for recrystallized and UFG-W are highlighted using solid symbols. Here the grain size  $d$  is a measure of the microstructural length scale, for grains and subgrains separated by both high-angle and low-angle boundaries.

gous temperatures ( $T < \sim 0.3T_m$ ,  $T_m$  being the melting temperature). Here, screw dislocations are the predominant carriers of plastic deformation, and the primary barrier to the motion of the screws is the lattice related Peierls potentials. The nucleation of kink pairs is the rate-limiting step controlling the dislocation mobility.<sup>15</sup> The operational activation volume of this process,  $v^*$ , is related to  $m$  as<sup>16,17</sup>

$$m = \frac{2kT}{\sigma v^*}. \quad (2)$$

For the kink-pair mechanism, at the high stresses encountered by a UFG material at high strain rates,  $v^*$  is in the order of a few  $b^3$  ( $b$  is the Burgers vector of the screw dislocation) and is almost independent of  $\sigma$ , or of  $d$ .<sup>16,18</sup> Therefore, at a given temperature  $T$  the  $m$  for a bcc metal would be approximately inversely proportional to the flow stress of the material. As such, by increasing  $\sigma$ , i.e., by reducing  $d$  and increasing dislocation density,  $m$  is substantially decreased. The W results are included in Fig. 3, which summarizes our previous experiments on bcc Fe, Ta, and V,<sup>13,19,20</sup> indicating that  $m$  would drop by up to a factor of 4–5 when the grain size is refined into the UFG regime.

Due to this combination of high strength and ductility, and the reduced role of stabilizing mechanisms (strain hardening and strain rate hardening), the UFG bcc microstructure will have an unprecedented low resistance to softening (thermal or geometric) mechanisms [see Eq. (1)]. Plastic flow will be more likely to localize in zones and bands, in which very high strains and strain rates are concentrated. This was indeed observed upon uniaxial high-rate compressive loading of the high-strength UFG-W. Figure 4(a) shows an optical micrograph of the UFG-W after loading at a strain rate of  $7500$   $s^{-1}$ . Two major shear zones, at an angle of approximately  $45^\circ$  relative to the loading direction, are clearly observed. A scanning electron image of a side face, with marked shear zones, is shown in Fig. 4(b). After polishing away the roughened surface followed by chemical etching, Fig. 4(c) shows clear evidence for the closely bundled plastic flow lines, as well as the subsequent incipient fracture. The

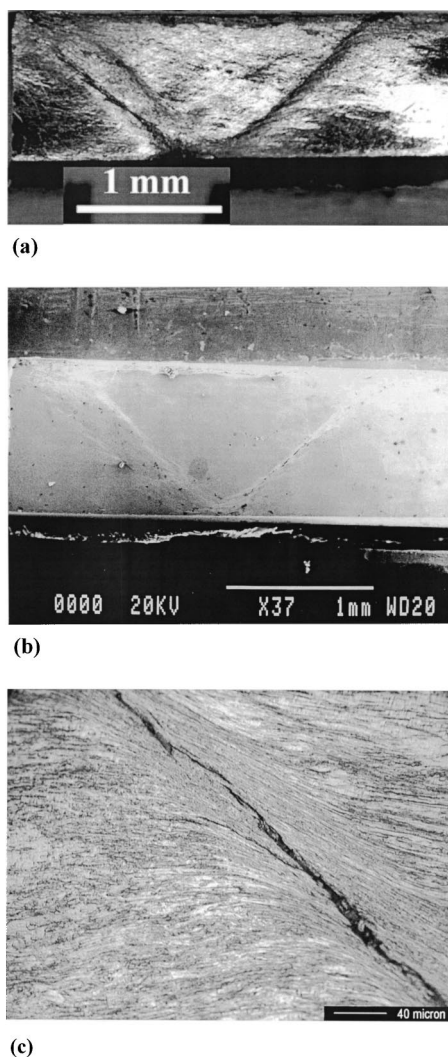


FIG. 4. (a) Optical and (b) scanning electron microscope images showing the shear zones, and (c) the intense concentrated plastic flow with crack initiation inside the shear zone.

latter, with crack formation in the desired location, is needed to discard material in the “self-sharpening” penetration,<sup>2,4</sup> and also partly responsible for the load drop seen in Fig. 2. None of the specimens showed barreling or other signs of significant frictional constraint. High-speed photography (not shown) indicated that the shear commences at a strain of  $\sim 0.1$ . Repeated Kolsky bar tests along different loading directions (e.g., in and perpendicular to the rolling plane) showed essentially the same behavior.

Conventional polycrystalline and warm-worked W (e.g., extrusion or swaging at 1200 °C) exhibits only uniform plastic deformation, with no sign of shear localization, under the same testing conditions. Also, it is common that cracks form parallel to the loading direction in these materials.<sup>12</sup> A main reason is the weakening effect of the impurities that segregate along the grain boundaries. In contrast, the UFG-W shows much enhanced ductility and no cracking even after large strains. SPD and grain refinement have improved the ductility simultaneously with strength, because the impurities redistribute to lower levels at the now numerous grain boundaries and other defects.<sup>10</sup> The dislocations added, particularly the large number of edge dislocations stored during low temperature SPD,<sup>21</sup> also promote the ductility.<sup>12,21,22</sup> A sufficiently high ductility is desirable, as early cracking at

small strains would preempt flow localization to release concentrated mechanical energy.

Until now, flow localization in W has been reported only when large artificial shear stresses are made possible by special designs in the sample geometry, hat-shaped or truncated cone-shaped samples being the most common.<sup>23,24</sup> The observation of shear localization in pure W reported here used Kolsky bar compression tests that do not involve significant barreling or frictional constraints. Based on the discussions above, flow localization should be promoted in other UFG bcc metals. This has indeed been observed, for example, in Fe and Ta.<sup>13,19,20,25</sup>

In summary, we have developed via SPD an ultrafine microstructure in commercial purity W. The resulting high strength and improved ductility, as well as reduced strain and strain rate hardening, lead to favorable conditions for the initiation of shear localization. This deformation mode observed in compression renders the high-density W uniquely suited for certain critical applications.

The authors thank Haitao Zhang and Tonia Jiao for experimental assistance and the support by ARL under the ARMAC-RTP Cooperative Agreement No. DAAD19-01-2-0003 at CAMCS.

<sup>1</sup>T. W. Wright, *The Physics and Mathematics of Adiabatic Shear Bands* (Cambridge University Press, Cambridge, 2002).

<sup>2</sup>L. S. Magness, D. Kapoor, and R. Dowding, *Mater. Manuf. Processes* **10**, 531 (1995).

<sup>3</sup>A. Bleise, P. R. Danesi, and W. Burkart, *J. Environ. Radioact.* **64**, 93 (2003).

<sup>4</sup>W. D. Cai, Y. Li, R. Dowding, F. A. Mohamed, and E. J. Lavernia, *Rev. Particulate Mater.* **3**, 71 (1995).

<sup>5</sup>J. J. Jonas, R. A. Holt, and C. E. Coleman, *Acta Metall.* **24**, 911 (1976).

<sup>6</sup>S. L. Semiatin and J. J. Jonas, *Formability and Workability of Metals* (ASM, 1984).

<sup>7</sup>D. Jia, Y. M. Wang, K. T. Ramesh, E. Ma, Y. T. Zhu, and R. Z. Valiev, *Appl. Phys. Lett.* **79**, 611 (2001).

<sup>8</sup>R. Z. Valiev, R. K. Islamgaliev, and I. V. Alexandrov, *Prog. Mater. Sci.* **45**, 103 (2000).

<sup>9</sup>K. T. Ramesh and R. S. Coates, *Metall. Trans. A* **23**, 2625 (1992).

<sup>10</sup>E. Lassner and W.-D. Schubert, *Tungsten-Properties, Chemistry, Technology of the Element, Alloys and Chemical Compounds* (Kluwer-Academic/Plenum, 1998).

<sup>11</sup>B. C. Allen, D. I. Maykuth, and R. I. Jaffee, *J. Inst. Met.* **90**, 120 (1962).

<sup>12</sup>A. M. Lennon and K. T. Ramesh, *Mater. Sci. Eng., A* **276**, 9 (2000).

<sup>13</sup>Q. Wei, T. Jiao, S. N. Mathaudhu, E. Ma, K. T. Hartwig and K. T. Ramesh, *Mater. Sci. Eng., A* **358**, 266 (2003).

<sup>14</sup>J. H. Bechtold, *Trans. AIME* **206**, 142 (1956); J. H. Bechtold and P. G. Shewmon, *Trans. ASME* **46**, 397 (1954).

<sup>15</sup>J. Marian, W. Cai, and V. V. Bulatov, *Nat. Mater.* **3**, 158 (2004).

<sup>16</sup>H. Conrad, in *High-Strength Materials*, edited by V. F. Zackay (Wiley, New York, 1965), p. 436.

<sup>17</sup>D. Caillard and J. L. Martin, *Thermally Activated Mechanisms in Crystal Plasticity* (Pergamon, Amsterdam, 2003), Chap. 2, p. 13.

<sup>18</sup>P. Rodriguez, *Metall. Mater. Trans. A* **35**, 2697 (2004).

<sup>19</sup>Q. Wei, S. Chen, K. T. Ramesh, and E. Ma, *Mater. Sci. Eng., A* **381**, 71 (2004).

<sup>20</sup>(a) D. Jia, K. T. Ramesh, and E. Ma, *Acta Mater.* **51**, 3495 (2003); (b) Q. Wei, L. Kecskes, T. Jiao, K. T. Hartwig, E. Ma, and K. T. Ramesh, *ibid.* **52**, 1859 (2004); (c) Q. Wei, Y. Jiao, K. T. Ramesh, and E. Ma, *Scr. Mater.* **51**, 367 (2004).

<sup>21</sup>H. Schultz, *Z. Metallkd.* **78**, 469 (1987).

<sup>22</sup>P. Gumbsch, J. Riedle, A. Hartmaier, and H. F. Fischmeister, *Science* **282**, 1293 (1998).

<sup>23</sup>T. Dummer, J. C. Lasalvia, G. Ravichandran, and M. A. Meyers, *Acta Mater.* **46**, 6267 (1998).

<sup>24</sup>J. R. Li, J. L. Yu, and Z. G. Wei, *Int. J. Impact Eng.* **28**, 303 (2003).

<sup>25</sup>Q. Wei, D. Jia, E. Ma, and K. T. Ramesh, *Appl. Phys. Lett.* **81**, 1240 (2002).